Improved micro x-ray fluorescence spectrometer for light element analysis

Stephan Smolek, Christina Streli, Norbert Zoeger, and Peter Wobrauschek
Atominstitut, Vienna University of Technology, Stadionallee 2, 1020 Vienna, Austria

(Received 18 February 2010; accepted 21 April 2010; published online 26 May 2010)

Since most available micro x-ray fluorescence (micro-XRF) spectrometers operate in air, which does not allow the analysis of low-Z elements ($Z \leq 14$), a special micro-XRF spectrometer has been designed to extend the analytical range down to light elements ($Z \geq 6$). It offers improved excitation and detection conditions necessary for light element analysis. To eliminate absorption of the exciting and fluorescent radiation, the system operates under vacuum condition. Sample mapping is automated and controlled by specialized computer software developed for this spectrometer. Several different samples were measured to test and characterize the spectrometer. The spot size has been determined by scans across a 10 μm Cu wire which resulted in a full width at half maximum of 31 μm for Mo Kα line (17.44 keV) and 44 μm effective beam size for the Cu K edge and 71 μm effective beam size for the Cu L edge. Lower limits of detection in the picogram range for each spot (or $\mu g/cm^2$) were obtained by measuring various thin metal foils under different conditions. Furthermore, detection limits in the parts per million range were found measuring NIST621 standard reference material. Area scans of a microscopic laser print and NaF droplet were performed to show mapping capabilities. © *2010 American Institute of Physics.* [doi:10.1063/1.3428739]

I. INTRODUCTION

Micro x-ray fluorescence (micro-XRF) is a well established tool to determine the spatial distribution of major, minor, and trace elements in a sample.[1–4] It is widely used to investigate samples from different fields (biology, geology, life science, etc.). The method is nondestructive, requires little sample preparation, and allows simultaneous multielement detection if an energy dispersive detector is used. Most available micro-XRF spectrometers operate in air which does not allow the analysis of low-Z elements ($Z \leq 14$). Preliminary testing using an existing vacuum chamber adapted to micro-XRF showed the possibility of this method for light element ($Z \geq 6$) analysis using a polycapillary x-ray optics.[5] Furthermore, the setup was tested using an air cooled low power x-ray tube (50 W) showing that this source is suited for micro-XRF analysis using a polycapillary.[6] However, the spectrometer had several significant drawbacks which prevented practical productive use: the polycapillary was mounted in a way that made it difficult to adjust and the optical microscope was not suited to adjust the sample accurately in respect to the beam. In order to solve these issues, a completely new spectrometer using some of the existing components has been designed. Emphasis lay on a simple, practical, compact, and extensible design. Components have been chosen in order to be able to perform micro-XRF on traditional fluorescence elements as well as light elements. The system is fully automated and computer controlled. That allows for long measurements to run without user interaction.

II. EXPERIMENTAL SETUP

The system uses an air cooled low power (50 kV, 1 mA, 50 W) Mo anode x-ray tube "Apogee" from Oxford XTG.[7] It has a small focal spot of 35 μm and a thin 125 μm Be window. This allows the use of the Mo L lines (Mo Lα 2.29 keV, Mo Lβ 2.39 keV) for particularly efficient excitation of the light elements. The small spot is ideal to be used in conjunction with a polycapillary optics. The x-ray generator is controlled via a computer interface.

The system uses an optics manufactured by XOS (Ref. 8) which has a total focal length of 128 mm and a nominal focal spot size of 32 μm for Mo Kα radiation. The gain factor in comparison to a 50 μm pinhole is 39. In order to adjust the optics it is mounted on a manual five-axis stage (x/y/z with 6 mm travel, θ/ϕ with $\pm 3°$ travel). This allows an easy adjustment of the optics in respect to the focal spot of the x-ray tube. Between the x-ray tube and the polycapillary, an optional beam filter can be set by means of a filter wheel.

The sample is mounted on a three-axis (x/y/z) motorized stage with 25 mm travel in each direction consisting of three Physik Instrumente PI M112.12S linear stages.[9] The resolution of the stages is less than 1 μm; movement is controlled via a computer interface. The sample holder is placed on a magnetic base that allows quick and easy mounting of the sample in the spectrometer. The sample is monitored using an optical microscope with a charge coupled device (CCD) camera. In order to position the sample accurately along the axis of the microscope, an objective with high depth resolution is needed. At the same time a long working distance is required from the microscope to be able to get the x-ray optics and the detector into position. The Mitutoyo M Plan Apo objective (10× magnification, depth resolution 3.5 μm, working distance 33.5 mm)[10] in conjunction with an Allied Vision "Marlin" high resolution CCD camera[11] is ideally suited for the task. The microscope is mounted on a manual three-axis (x/y/z) stage for adjustment relative to the sample.

The fluorescence radiation from the sample is detected by means of a Si(Li) detector (Gresham) with an active area

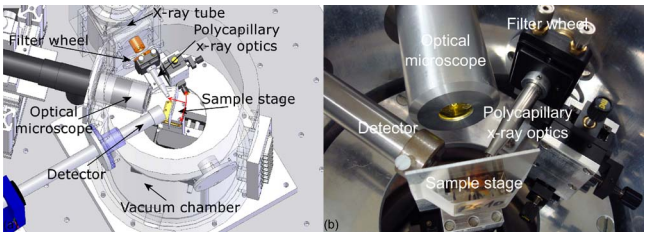

FIG. 1. (Color online) CAD design rendering and photo of the interior of the spectrometer. The polycapillary is five-axis adjustable; the microscope looks into the chamber through a 8 μm Kapton™ window; the detector is moved as close as possible to the sample; the sample can be automatically moved in x/y/z.

of 30 mm^2. It features an ultrathin 300 nm polymer window (AP1.4) (Ref. 12) that allows low energy photons to be detected. A collimator and electron trap are placed at the tip of the detector snout. The signal is amplified and shaped by a Tracor 1255 amplifier before it is sent into an Amptek MCA8000A multichannel analyzer.[13]

The whole setup is placed inside a custom cylindrical vacuum chamber made at the Atominstitut. The advantages of putting the system into vacuum are no absorption of the primary and fluorescence radiation between x-ray tube, sample, and detector and no Ar peaks in the spectrum. The x-ray tube is mounted directly onto the chamber (vacuum tight). The microscope has to be in air and looks into the chamber through an 8 μm Kapton™ window inside a small pot so that it is close enough to the sample. The detector snout enters the chamber through a flange that allows the detector crystal to be placed as close as possible to the sample. The sample stage is mounted on a double bottom floor plate to reduce influence of bending of the chamber floor under vacuum condition. The adjustment stage for the polycapillary is mounted on a raised ring plate inside the chamber. The inside of the chamber is accessible from the top after removing the lid. A 10-mm-thick glass window in the lid allows the operator to observe the sample positioning in addition to the microscope image. Due to the fact that the detector is light sensitive, a second lid has to be placed over the window during x-ray measurements. A safety switch at the lid deactivates the x-ray generator should it be removed while the x-ray beam is on. This, in conjunction with the closed vacuum chamber, makes the spectrometer inherently protected. The setup can be seen in Fig. 1.

The measurement process is computer controlled by specialized computer software developed specifically for this spectrometer at the Atominstitut (Fig. 2). It controls the sample stage, the spectrum acquisition process, and the x-ray generator. The microscope image is also displayed at the computer. A crosshair overlay enables precise positioning of the sample relative to the beam. Microscope images can also be saved. The software can automatically perform scans (line scans or areas cans) of a sample to determine the special distribution of elements. Multiple scans can be programmed and processed. Automatic region of interest (ROI) evaluation of the measured spectra is performed (with preprogrammed ROIs) and the resulting maps are displayed as a live preview. For every point the full spectrum is saved for further evaluation, for example spectral line deconvolution with an appropriate software package (e.g., QXAS, IAEA).[14]

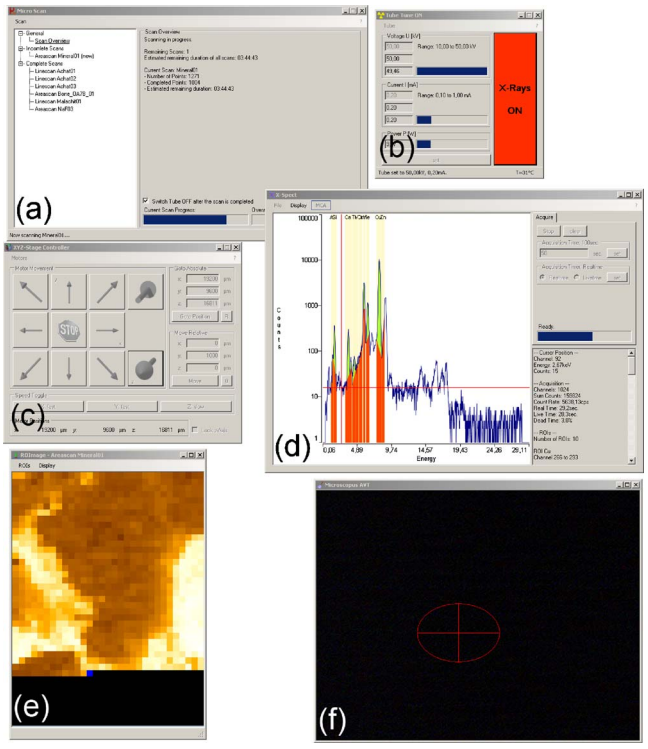

FIG. 2. (Color online) Screenshot of the measurement software controlling (a) the scanning process, (b) the x-ray generator, (c) the sample stage movement, (d) spectrum acquisition and ROI evaluation, (e) creating live ROI maps, and (f) showing the microscope image with a crosshair overlay.

III. RESULTS

Various samples were measured to test and characterize the spectrometer. The minimum beam diameter was searched and the spatial resolution checked by scanning across a 10 μm Cu wire. Knowing the full width at half maximum (FWHM) of the scan profile and the wire diameter the beam size (FWHM of the beam profile) can be estimated by the following formula:[15]

$$\mathrm{FWHM}_{\mathrm{beam}} \approx \sqrt{\mathrm{FWHM}^2_{\mathrm{profile}} - d^2_{\mathrm{wire}}}.$$

The critical angle of total reflection inside the polycapillaries is a function of the photon energy[16]

$$\varphi_c \approx \frac{28.8}{E}\sqrt{\frac{Z\rho}{A}}.$$

Here ϕ_c is the critical angle (millirad), E is the photon energy (keV), ρ the density $[\mathrm{g/cm}^3]$, Z is the atomic number, and A is the atomic mass. For photons with a higher energy (e.g., Mo Kα) the critical angle is small. Each capillary focuses the radiation nicely into the focal spot of the optics; the divergence of the beam coming out of a single capillary is small. For low energy radiation (e.g., Mo Lα), the critical angle is large; therefore, the divergence of the beam of a single capillary is also large. The result is a larger beam diameter.

Since the spectrometer uses polychromatic excitation knowing the resolution for different chemical elements is

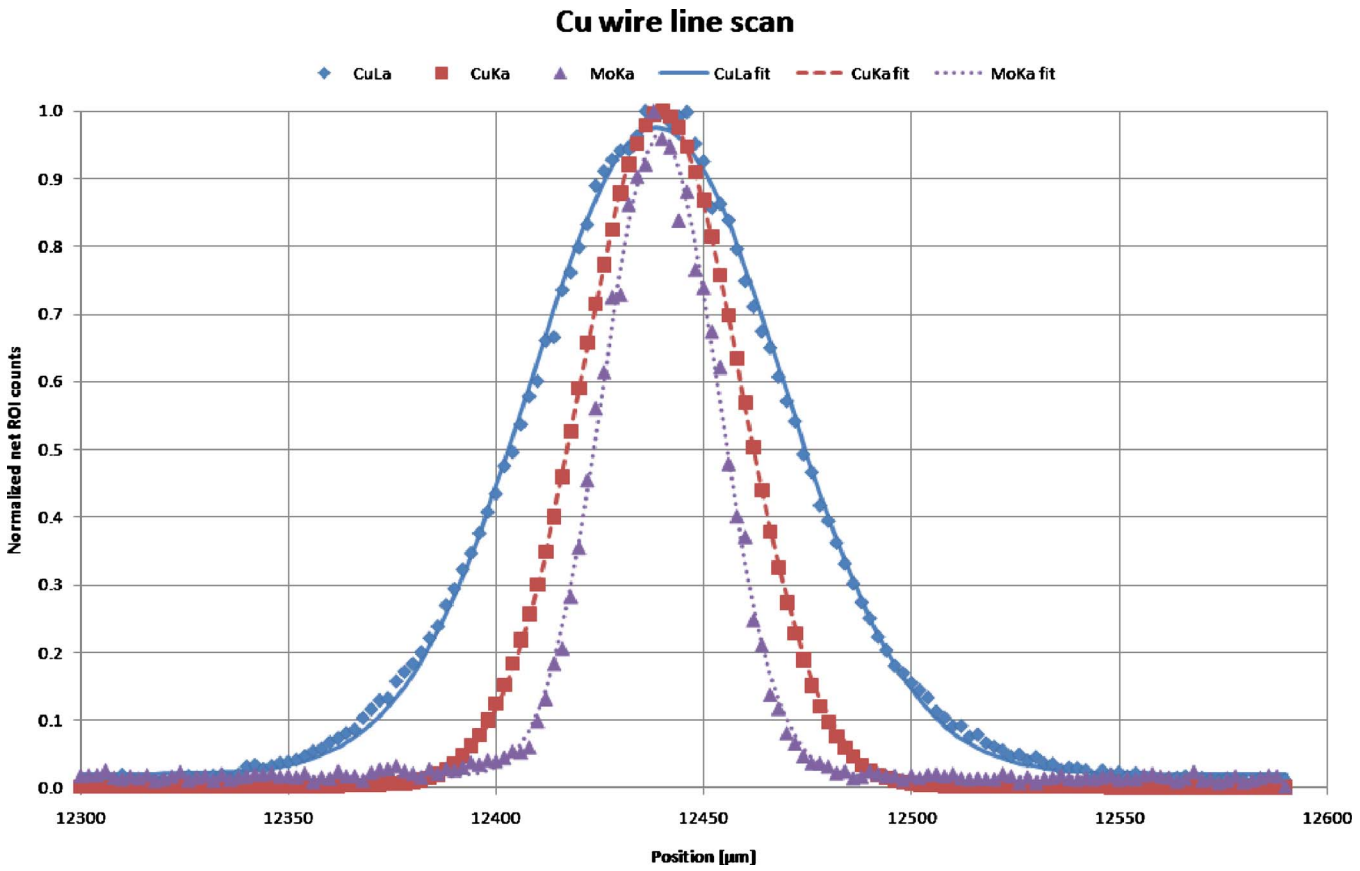

FIG. 3. (Color online) Measured scan profiles and Gaussian fits from a line scan across a 10 μm Cu wire for the Cu Lα and Cu Kα lines as well as the Mo Kα scatter peak.

important. Using the Mo Kα scatter peak, the Cu Kα and the Cu Lα fluorescence lines the beam diameter can be determined across a wide energy range in one experiment. If the spot size is measured by means of fluorescence radiation, it is determined for an effective average energy $\langle E \rangle$ of all x rays above the corresponding absorption edge.[17] As the energy dependent transmission function for the polycapillary is not known, calculating $\langle E \rangle$ is not really possible. It is only possible to say that the spot size is determined for the chemical element and specific absorption edge of the wire material. Figure 3 shows the experimental result: for the Mo Kα (17.44 keV) scatter radiation the spot size is about 31 μm. This is in good agreement to the nominal focal spot size of 32 μm stated by the manufacturer (XOS). The effective beam diameter for the Cu K edge (8.98 keV) is about 44 μm and for Cu L edge (1.1 keV) about 71 μm. The error of this measurement comes mainly from the uncertainty of the wire diameter ($\pm 10\%$). The statistics contributes only in the range of 1%.

In order to find the minimum spot size the Cu wire was scanned at different positions along the beam axis. This measurement also yields information about the sensitivity of spatial resolution the system to slight changes in position along the beam axis. This is important as the position along the beam axis is controlled by the depth resolution of the optical microscope. Figure 4 shows the result of this scan for the beam size at the Cu K edge (Cu Kα radiation). The beam size is stable across a length of about 200 μm in the beam axis.

Another important characteristic of an x-ray fluorescence spectrometer is the sensitivity. To calculate lower limits of detection, thin metal foils were used. Knowing the effective diameter of the beam on the sample surface d and the foil thickness x it is possible to calculate the amount of mass that is being excited in the sample (with the density of the foil material ρ)

$$m = \frac{\pi}{2} d^2 x \rho.$$

Neglecting self absorption in the sample the lower limits of detection can be calculated as

$$\mathrm{LLD} = m \frac{3\sqrt{N_B}}{N_N},$$

where N_B are the background counts and N_N are the net peak area counts. The acquisition time was set to 1000 s live time. To be able to compare results obtained with different tube currents, the result was normalized to 1 mA. Table I summarizes the obtained results. One can see that the lower limits of detection are in the picogram range. Different tube currents (and therefore low and high detector dead times) have no significant influence on the detection limits, as can be seen from the Ni foil measurements. The result for Al depends strongly on the mode of excitation. If the Mo L lines are removed from the beam by means of a 100 μm Al filter, the detection limits are a factor 10 higher in comparison to excitation with the L-lines. On the other hand, there is almost

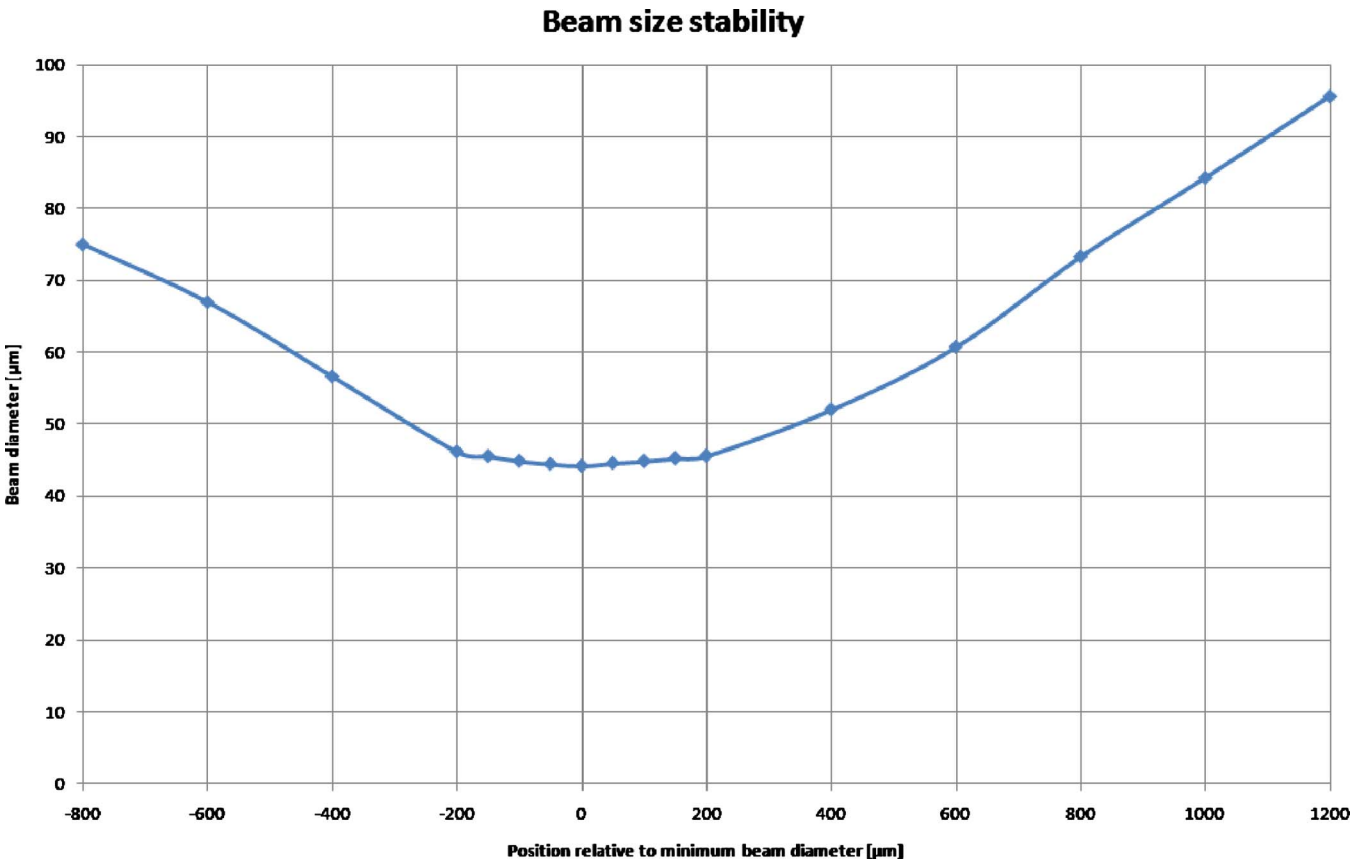

FIG. 4. (Color online) Measured beam diameter at the Cu K edge for different positions along the beam axis to determine beam size stability.

no difference between excitation with 20 or 50 kV for Al. The detection limit of Au, which is detected via the L-lines, is about a factor two higher. Note that these detection limits refer to the amount of mass in one spot! For better comparison the obtained values were normalized to one square centimeter. Results show detection limits below 1.5 $\mu g/cm^2$ or 10^{16} atoms/cm^2 (higher with Al filter).

A standard reference material (NIST 621 soda-lime container glass) has been measured to obtain further information about the lower limits of detection. To compensate for any inhomogeneities, an area scan rather than a single point measurement has been performed with a total acquisition live time of 1000 s. The sum spectrum of the scan (Fig. 5) has been used to calculate lower limits of detection. The sample was measured with and without a 100 μm Al beam filter. The results are in the ppm range. For the light elements results are better without the Al filter. Table II shows the obtained detection limits. For Na, the limit is below 1000 ppm; for Si about 100. Ti, Fe, As, and Zr have limits of about 10 ppm.

To show mapping capabilities several different samples have been measured. An artificial elemental distribution was created by printing the miniature text "ATI" (abbreviation for Atominstitut) using a standard laser printer on normal printer paper. The printer toner contains small amounts of copper. The sample was scanned with 40 μm steps and 150 s real time each point. A size comparison of the sample with a one cent coin and the scan result can be seen in Fig. 6. While the

TABLE I. Lower limits of detection in one spot for various elements under different measurement conditions.

Sample properties			X-ray tube parameters			Lower limits of detection		
Element	Beam diameter (μm)	Thickness (μm)	V (kV)	I (mA)	Filter	Per spot (pg)	Per area ($\mu g/cm^2$)	Per area (atoms/cm^2)
Ni	44	4	50	0.1	100 μm Al	11	0.5	5×10^{15}
Ni	44	4	50	0.4	100 μm Al	13	0.6	6×10^{15}
Ni	44	4	50	1	100 μm Al	14	0.7	7×10^{15}
Zn	44	4	50	0.4	100 μm Al	10	0.5	4×10^{15}
Al	70	0.8	50	1	100 μm Al	102	1.9	4×10^{16}
Al	70	0.8	50	1	None	8	0.1	3×10^{15}
Al	70	0.8	20	1	None	7	0.1	3×10^{15}
Au	40	1	50	0.4	100 μm Al	25	1.4	4×10^{15}

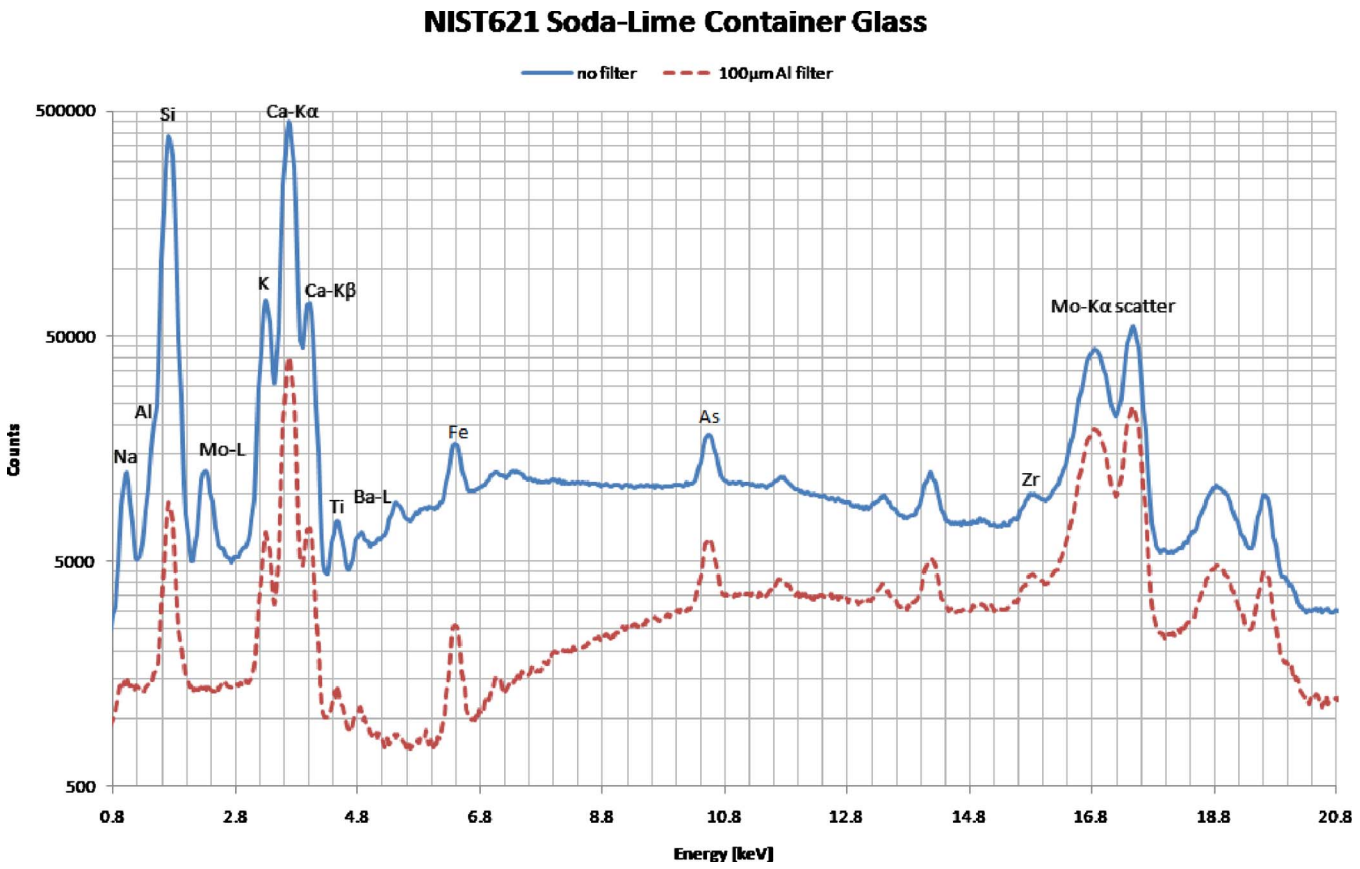

FIG. 5. (Color online) Sum spectra of NIST621 soda-lime container glass with and without filter. Measurement conditions: 50 kV, 1 mA, 1000 s live time acquisition.

Ca distribution from the paper shows no sign of the text, it is clearly visible on the micro-XRF image of the Cu distribution.

An area scan of dried residue of a NaF droplet (10 μl, 100 ppm) on a Kapton™ foil was performed to show mapping capabilities of light elements. Mo L excitation was used for this sample with the x-ray tube set to 20 kV, 1 mA. Scanning step width was 40 μm and measurement time was 100 s real time for each point. Figure 7 shows the area scan image as well as a sample spectrum showing the Mo L excitation of NaF.

TABLE II. Lower limits of detection obtained with the NIST 621 standard reference material for different excitation modes.

Element	LLD (ppm)	LLD (100 μm Al filter) (ppm)
Na	878	36 409
Al	115	4898
Si	95	2513
K	22	148
Ca	15	81
Ti	8	17
Fe	5	6
As	4	5
Zr	2	4
Ba	54	145

IV. CONCLUSIONS

An improved micro-XRF spectrometer for light element analysis has been designed, characterized and tested with various samples. The system consists of a low power Mo anode x-ray tube, a polycapillary x-ray optics, motorized sample stage, high resolution CCD microscope, and a Si(Li) detector with thin window. The setup is placed inside a vacuum chamber to avoid absorption of the primary radiation (also the Mo L lines) and the low energy fluorescent radiation. The spectrometer offers a resolution of 71 μm for the Cu L edge, 44 μm for the Cu K edge, and 31 μm for Mo Kα radiation. This is important for quantitative calculations of different elements with polychromatic excitation as different areas are illuminated. Lower limits of detection are in the picogram range for each spot (or $\mu g/cm^2$) and in the parts per million range, respectively. Mapping of light elements has been demonstrated using a NaF droplet area scan. The spectrometers design allows for future extensions (con-

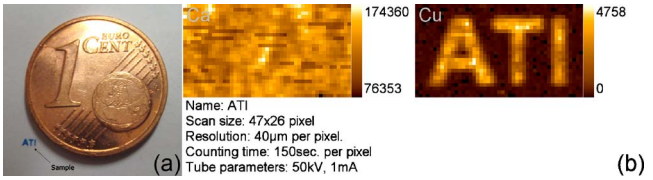

FIG. 6. (Color online) (a) Laser print "ATI" size comparison with a one cent coin and (b) scan result for Ca (Paper) and Cu (Toner).

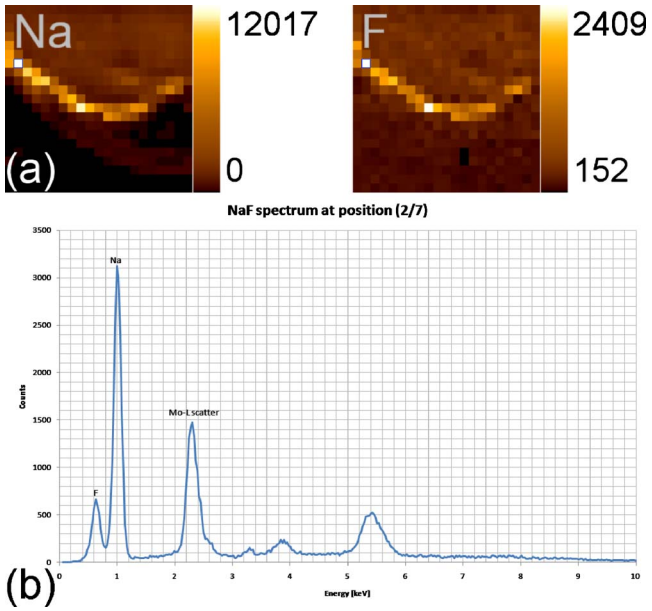

FIG. 7. (Color online) (a) Area scan of a NaF droplet residue (21×21 pixel, 40 μm steps, 100 s RT, 20 kV, 1 mA) and (b) spectrum of position (2/7) showing efficient Mo L excitation of Na and F.

focal, tomography) to be implemented. Access to the spectrometer is available for external users through the transnational access program of a running European Commission infrastructure project (ANNA, www.i3-anna.org).

ACKNOWLEDGMENTS

This work was supported by the "Innovative Projekte" funds of the TU Wien and the ANNA project. Special thanks to Walter Drabek for building the mechanical components.

[1] A. Rindby, X-Ray Spectrom. **22**, 187 (1993).
[2] S. Bichlmeier, K. Janssens, J. Heckel, D. Gibson, P. Hoffmann, and H. M. Ortner, X-Ray Spectrom. **30**, 8 (2001).
[3] S. A. Hoffman, D. J. Thiel, and D. H. Bilderback, Nucl. Instrum. Methods Phys. Res. A **347**, 384 (1994).
[4] B. Vekemans, K. Janssens, G. Vittiglio, F. Adams, L. Andong, and Y. Yiming, JCPDS Card No. 278–290 (1999).
[5] C. Streli, N. Marosi, P. Wobrauschek, and B. Frank, Rigaku J. **20**, 25 (2003).
[6] P. Wobrauschek, B. Frank, N. Zoeger, C. Streli, N. Cernohlawek, C. Jokubonis, and H. Hoefler, Adv. X-ray Anal. **48**, 229 (2005).
[7] See www.oxfordxtg.com for x-ray tubes.
[8] See www.xos.com for polycapillary x-ray optics.
[9] See www.physikinstrumente.com for micro translation stages.
[10] See www.mitutoyo.co.jp for microscope objectives.
[11] See www.alliedvisiontec.com for CCD cameras.
[12] See www.moxtek.com for detector windows.
[13] See www.amptek.com for multi channel analyzers.
[14] See http://www.iaea.org/OurWork/ST/NA/NAAL/pci/ins/xrf/pciXRFdown.php for XRF software downloads.
[15] K. Proost, L. Vincze, K. Janssens, N. Gao, E. Bulska, M. Schreiner, and G. Falkenberg, X-Ray Spectrom. **32**, 215 (2003).
[16] P. Kregsamer, C. Streli, and P. Wobrauschek, *Handbook of X-Ray Spectrometry*, 2nd ed., edited by R. Van Grieken and A. Markowicz (Dekker, New York, 2002), p. 564.
[17] N. Gao and K. Janssens, *X-Ray Spectrometry: Recent Technological Advances*, edited by K. Tsuji, J. Injuk, and R. Van Grieken (Wiley, New York, 2004), p. 95.